

Quantum fluctuations in one-dimensional arrays of condensates

Alessandro Cuccoli, Andrea Fubini, Valerio Tognetti

Dipartimento di Fisica dell'Università di Firenze and Istituto Nazionale di Fisica della Materia (INFM),
Largo E. Fermi 2, I-50125 Firenze, Italy

Ruggero Vaia

Istituto di Elettronica Quantistica del Consiglio Nazionale delle Ricerche, via Panciatici 56/30, I-50127 Firenze, Italy,
and Istituto Nazionale di Fisica della Materia (INFM)
(December 20, 2018)

The effects of quantum and thermal fluctuations upon the fringe structure predicted to be observable in the momentum distribution of coupled Bose-Einstein condensates are studied by the effective-potential method. For a double-well trap, the coherence factor recently introduced by Pitaevskii and Stringari (cond-mat/0104458) is calculated using the effective potential approach and is found in good agreement with their result. The calculations are extended to the case of a one-dimensional array of condensates, showing that quantum effects are essentially described through a simple renormalization of the energy scale in the classical analytical expression for the fringe structure. The consequences for the experimental observability are discussed.

Recently, extensive theoretical work was devoted to the problem of the coherence properties arising from the interaction among two or more trapped condensates^{1–3}. These effects are experimentally accessible⁴ and can be considered of the same nature as in Josephson junctions⁵. As a matter of fact, the condensates can be characterized by their phases $\hat{\varphi}_i$ and atom numbers \hat{n}_i , which are conjugate canonical variables satisfying $[\hat{\varphi}_i, \hat{n}_j] = i \delta_{ij}$. The Hamiltonian looks indeed like the Josephson one^{5,6}, namely

$$\hat{\mathcal{H}} = \frac{E_c}{4} \sum_{i=1}^{N_s} \hat{n}_i^2 - E_j \sum_{\langle ij \rangle} \cos(\hat{\varphi}_i - \hat{\varphi}_j), \quad (1)$$

for an array of N_s condensates, where the second summation runs over the nearest-neighbor condensates. For two interacting condensates ($i = 1, 2$) this reduces to

$$\hat{\mathcal{H}}_0 = \frac{E_c}{2} \hat{n}^2 - E_j \cos \hat{\varphi} \quad (2)$$

with $\hat{n} = (\hat{n}_1 - \hat{n}_2)/2$ and $\hat{\varphi} = \hat{\varphi}_1 - \hat{\varphi}_2$. The interaction parameters E_c and E_j depend on the chemical potential and the wave-function overlap of neighboring condensates, respectively⁵. For the above Hamiltonians it is convenient to define a quantum coupling parameter g as the ratio between the quantum energy scale $\hbar\omega_0 = \sqrt{E_c E_j}$ of the quasi-harmonic excitations and the overall energy scale of the nonlinear interaction, E_j , so that quantum effects are weak (strong) for

$$g = \sqrt{E_c/E_j} \quad (3)$$

small (large) compared to 1. The temperature is also conveniently measured in the scale of E_j by the dimensionless parameter $t \equiv T/E_j$.

For the two-condensate case, starting from the uncertainty principle $\langle \Delta \hat{n}^2 \rangle \langle \Delta \sin^2 \hat{\varphi} \rangle \geq (\hbar^2/4) \langle \cos \hat{\varphi} \rangle$, the authors of Ref. 2 introduced the *coherence factor*

$$\alpha(g, t) = \langle \cos \hat{\varphi} \rangle, \quad (4)$$

a parameter that can be directly related with the fringe structure in momentum space, which is due to the onset of coherence between the weakly linked condensates and can be detected by light scattering experiments. Indeed, the observed momentum distribution $n(\mathbf{p})$ turns out to be described, in terms of the single-condensate distribution $n_0(\mathbf{p})$, as^{2,3} $n(\mathbf{p}) = 2 [1 + \alpha(g, t) \cos(p_x d/\hbar)] n_0(\mathbf{p})$, where d is the distance of the condensate traps (assumed along the x -axis). In an analogous way, purely quantum mechanical correlations between identical particles lead to a reduction of the neutron scattering intensity of protons or deuterons which can be explained by a similar mechanism⁷. At zero temperature, $1 - \alpha$ measures the decoherence effect of the only zero-point quantum fluctuations. The value $\alpha = 1$ occurs when the quantum coupling $g = 0$ and corresponds to the classical limit, while α decreases for increasing values of g . When the temperature is finite, α decreases further due to the thermal fluctuations that contribute to the destruction of coherence. This thermal decoherence turned out to be significant even at very low temperatures where the condensation starts to occur, as shown in Ref. 3 for the single BEC junction. However, the analogous calculation for an array of condensates, that involves the phase correlation function

$$G_r(g, t) = \langle \cos(\hat{\varphi}_i - \hat{\varphi}_{i+r}) \rangle, \quad (5)$$

cannot be obtained by a direct numerical solution of the Schrödinger equation, as done in Ref. 3.

We note that an ideal tool to face such calculations is represented by the effective potential method⁸. Several applications⁹ proved indeed its usefulness: in particular, it can be used for one- (1D) and two-dimensional (2D) arrays¹⁰, where, otherwise, the exact quantum solution can be obtained only by resorting to much heavier quantum Monte Carlo simulations. The method is a semiclassical expansion in terms of the quantum coupling $g = \sqrt{E_c/E_j}$. The only pure-quantum part of the fluc-

tuations is considered in the self-consistent Gaussian approximation so that the quantum Hamiltonian is reduced to a classical-like one, where the parameters of the potential are renormalized by the pure-quantum effects at any temperature. Of course this renormalization vanishes at high temperatures, ($\beta = 1/T \rightarrow 0$), the approximation thus being more and more accurate.

Let us first consider the *two-condensate case*. The renormalization parameter which takes into account the quantum fluctuations only, is related to the pure-quantum Gaussian spread of the phase; it turns out to be

$$D_0(g, t) = \Delta\hat{\varphi}_{\text{tot}}^2 - \Delta\hat{\varphi}_{\text{class}}^2 = \frac{g}{2\kappa_0} \left(\coth f - \frac{1}{f} \right), \quad (6)$$

where $f(g, t) = \beta\hbar\omega/2 = g\kappa_0/(2t)$ and the renormalized frequency is $\omega = \kappa_0\omega_0$; the *pure-quantum* Hartree factor⁹

$$\kappa_0(g, t) = e^{-D_0(g, t)/4} \quad (7)$$

is determined self-consistently with $D_0(g, t)$, which is a decreasing function of temperature and vanishes for $t \rightarrow \infty$. The effective classical Hamiltonian⁹ corresponding to Eq. (2) bears the same functional form,

$$\mathcal{H}_0 = \frac{E_C}{2} n^2 - E_J \kappa_0^2(g, t) \cos \varphi, \quad (8)$$

with the renormalized Josephson coupling $E_J \kappa_0^2(g, t)$ (some additive uniform terms, which do not affect the calculation of thermal averages, have been neglected). In the effective potential formalism any quantum average is evaluated by means of a classical-like expression, that for the case of the coherence factor reads

$$\alpha(g, t) = \frac{1}{Z_C} \int d\varphi (\kappa_0^2 \cos \varphi) \exp \left[\frac{\kappa_0^2}{t} \cos \varphi \right], \\ = \kappa_0^2 \mathcal{I}_0(\kappa_0^2/t), \quad (9)$$

where \mathcal{I}_0 is the logarithmic derivative of the modified Bessel function of the first kind $I_0(x)$:

$$\mathcal{I}_0(x) = \frac{d \ln I_0(x)}{dx} = \frac{I_1(x)}{I_0(x)}. \quad (10)$$

For $g = 0$ one has $\kappa_0(0, t) = 1$ and Eq. (9) reduces to the exact classical coherence factor $\alpha_{\text{cl}}(t) = \mathcal{I}_0(1/t)$, while it is worthwhile to notice that within our approximation quantum effects are described by a renormalization of the temperature scale. The results are reported for different quantum-coupling values in Fig. 1, where comparison with the exact ones is made. It appears that the method is reliable as long as the renormalizations are small, $D_0 \lesssim 1$. Note that D_0 is a decreasing of t , so this condition is verified also at strong coupling if t is high enough, while the validity in the whole temperature range requires $D_0(g, 0) \lesssim 1$, i.e. $g \lesssim 1.5$. The result for $g = 1$ is in very good agreement with the corresponding one of Ref. 3 in the whole temperature range, while, as

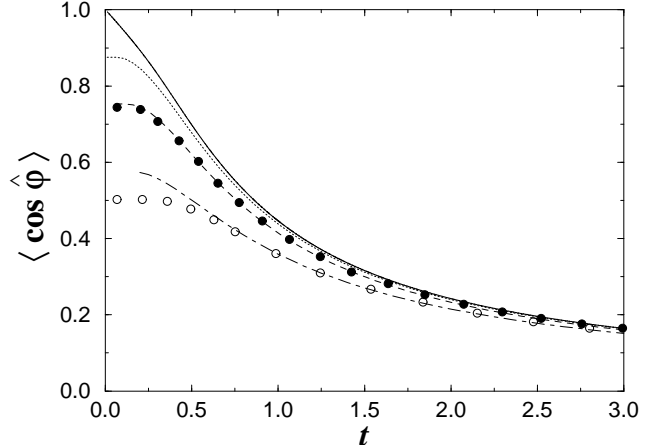


FIG. 1. Coherence factor $\alpha(g, t) = \langle \cos \varphi \rangle$, Eq.(4). Solid line: $g = 0$ (classical); dotted line: $g = 0.5$; dashed line: $g = 1$; dash-dotted line: $g = \sqrt{3}$. The symbols are the exact result² for $g = 1$ (full circles) and $g = \sqrt{3}$ (open circles). The latter value corresponds to $E_C/E_J = 3$.

expected, the result for $g = \sqrt{3}$ matches the exact data for $t \gtrsim 0.5$. This testifies to the reliability of the method, which can be then pursued also for condensate arrays, where quantum fluctuations are expected to be weaker.

Let us now come to the case of a *1D condensate array*. The effective Hamiltonian corresponding to Eq. (1) reads

$$\mathcal{H} = \sum_{i=1}^{N_S} \left[\frac{E_C}{4} n_i^2 - E_J \kappa^2(g, t) \cos(\varphi_i - \varphi_{i+1}) \right], \quad (11)$$

where now the pure-quantum Hartree factor is given by

$$\kappa(g, t) = e^{-\mathcal{D}_1(g, t)/4}, \quad (12)$$

and is to be self-consistently evaluated together with the renormalization parameter

$$\mathcal{D}_1(g, t) = \frac{g}{2\sqrt{2}\kappa} \sum_k \left| \sin \frac{k}{2} \right| \left(\coth f_k - \frac{1}{f_k} \right), \quad (13)$$

which is a decreasing function of t since

$$f_k(g, t) = \frac{\beta\hbar\omega_k}{2} = \frac{g\kappa}{\sqrt{2}t} \left| \sin \frac{k}{2} \right|; \quad (14)$$

indeed, the renormalized dispersion relation takes the form $\hbar\omega_k = \sqrt{2}\kappa\omega_0 |\sin(k/2)|$. The approximation holds if $\mathcal{D}_1(g, t) \lesssim 1$, and since at zero temperature $\mathcal{D}_1(g, 0) = g/(\sqrt{2}\pi\kappa)$, the condition amounts to require $g \lesssim 3.5$.

For the correlation function (5) the effective-potential recipe gives¹¹

$$G_r(g, t) = e^{-\mathcal{D}_r/2} [\mathcal{I}_0(\kappa^2/t)]^{|r|}, \quad (15)$$

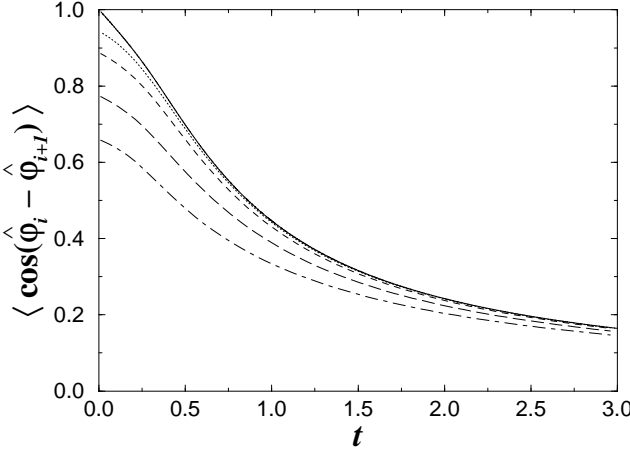


FIG. 2. Nearest-neighbor correlation function of the 1D condensate chain $G_1(g, t) = \langle \cos(\hat{\varphi}_i - \hat{\varphi}_{i+1}) \rangle$, Eq.(17). Solid line: $g = 0$ (classical); dotted line: $g = 0.5$; short-dashed line: $g = 1$; long-dashed line: $g = 2$; dash-dotted line: $g = 3$.

with $\mathcal{I}_0(x)$ as in Eq. (10); the analytical evaluation uses periodic boundary conditions and the translation invariance of the potential¹¹. The renormalization parameters for the r -th neighbors read

$$\mathcal{D}_r(g, t) = \frac{g}{2\sqrt{2}\kappa} \frac{1}{N_s} \sum_k \frac{\sin^2(rk/2)}{|\sin(k/2)|} \left(\coth f_k - \frac{1}{f_k} \right); \quad (16)$$

for $r \rightarrow \infty$ one can replace $\sin^2(rk/2)$ by its average $1/2$ and get the asymptotic value $\mathcal{D}_\infty(g, t)$ which is logarithmically divergent for $t = 0$. In particular one has the power-law asymptotic behavior $e^{-\mathcal{D}_\infty(g, t)/2} \sim t^\eta$, with $\eta = g/[4\sqrt{2}\pi\kappa(g, 0)] = \mathcal{D}_1(g, 0)/4$. Moreover, the zero- t correlation function behaves as $G_r(g, 0) = e^{-\mathcal{D}_r(g, 0)/2} \sim r^{-\eta}$ in agreement with the theoretical prediction for the low-coupling phase¹².

For the first-neighbor correlation, we can define the analog of the coherence factor, Eqs. (4), which in the effective-potential approximation bears the same form of Eq. (9),

$$\langle \cos(\hat{\varphi}_i - \hat{\varphi}_{i+1}) \rangle = \kappa^2 \mathcal{I}_0(\kappa^2/t); \quad (17)$$

it is plotted in Fig. 2. It appears that the quantum correction is weaker compared to the two-condensate case. It is worthwhile to notice that in the classical case, i.e. $g = 0$, Eq. (15) reduces to the correct classical expression.

The formulas above can also be easily generalized¹⁰ to the 2D case, of recent experimental realization¹³, but the involved classical-like integrals cannot be evaluated analytically as in Eq. (15), so a numerical approach is needed, e.g. Monte Carlo (MC) simulation (still much easier than quantum MC).

For the multi-condensate array (with spacing d along the x -direction) the momentum distribution $n(\mathbf{p}) = N_s n_0(\mathbf{p}) \Xi(p_x)$ exhibits a fringe structure determined by the structure function

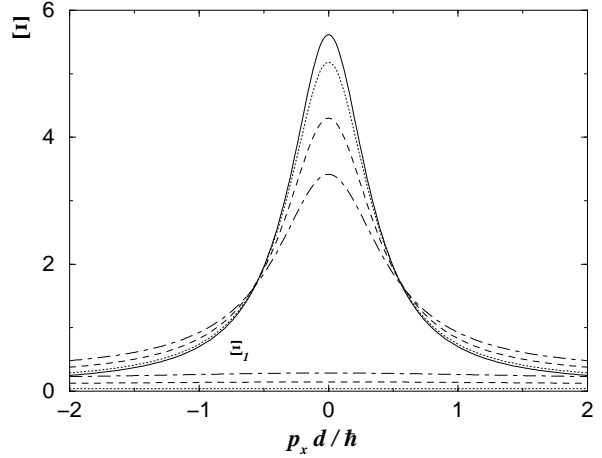


FIG. 3. Structure function $\Xi(p_x; g, t)$ of the 1D condensate chain [Eq.(19)] at fixed $t = 0.5$. Solid line: $g = 0$ (classical); dotted line: $g = 0.5$; short-dashed line: $g = 1$; long-dashed line: $g = 2$; dash-dotted line: $g = 3$. The low-lying curves report the small contribution of the term $\Xi_1(p_x; g, t)$ for the same values of g . One single periodic interval is displayed.

$$\begin{aligned} \Xi(p_x) &\equiv \sum_r e^{-irp_x d/\hbar} \langle \cos(\hat{\varphi}_i - \hat{\varphi}_{i+r}) \rangle \\ &= \sum_r e^{-irp_x d/\hbar} e^{-\mathcal{D}_r/2} [\mathcal{I}_0(\kappa^2/t)]^{|r|}, \end{aligned} \quad (18)$$

where Eq. (15) has been inserted; clearly, $\Xi(p_x) = \Xi(p_x + 2\pi\hbar/d)$ is periodic. In this expression one can take advantage of the fact that the renormalization coefficients $\mathcal{D}_r(g, t)$ rapidly converge to the asymptotic value $\mathcal{D}_\infty(g, t)$, separating it as

$$\Xi(p_x) = \Xi_0(p_x) + \Xi_1(p_x), \quad (19)$$

$$\Xi_0(p_x) = e^{-\mathcal{D}_\infty/2} \frac{1 - \alpha^2}{1 + \alpha^2 - 2\alpha \cos(p_x d/\hbar)} \quad (20)$$

$$\Xi_1(p_x) = \sum_r e^{-irp_x d/\hbar} \alpha^{|r|} (e^{-\mathcal{D}_r/2} - e^{-\mathcal{D}_\infty/2}) \quad (21)$$

where the quantity

$$\alpha(g, t) = \mathcal{I}_0(\kappa^2(g, t)/t), \quad (22)$$

characterizes the coherence effect. Looking at Eq. (21) it appears that the difference in parentheses cuts off the contribution from large values of r , so this term does not show sharp features and the fringe structure is mostly given by Eq. (20). In the classical limit ($g = 0$) $\mathcal{D}_r = 0$ vanishes and so does $\Xi_1(p_x)$, and the exact classical result³ is immediately recovered since $\alpha(0, t) = \alpha_{\text{cl}}(t)$.

Representative results for the full structure function $\Xi(p_x)$ and the correction $\Xi_1(p_x)$ are reported in Fig. 3 for some values of the quantum coupling g at fixed temperature $t = 0.5$. The stronger the quantum effects (i.e., high g and low t) the higher is $\Xi_1(p_x)$, but in the considered parameter range the relative contribution of $\Xi_1(p_x)$ is small and broad, confirming that the main structure is contained in $\Xi_0(p_x)$. In Fig. 4 the structure function $\Xi(g, t)$ is plotted for fixed $g = 1$ and different temperatures, in a wider range of p_x so to display the periodic behavior.

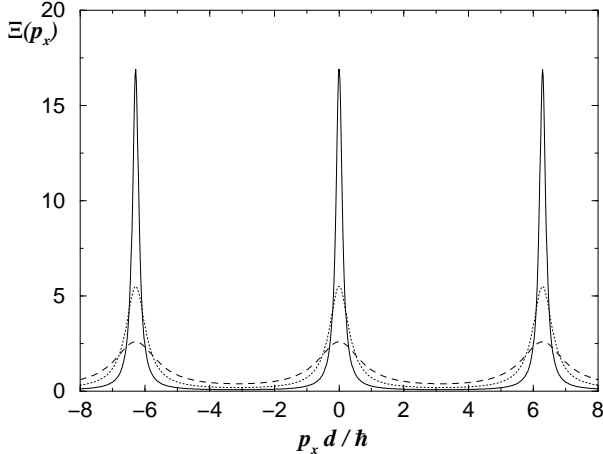


FIG. 4. Structure function $\Xi(p_x; g, t)$ of the 1D condensate chain [Eq.(19)], at fixed $g = 0.5$. Solid line: $t = 0.2$; dotted line: $t = 0.5$; dashed line: $t = 1$.

Finally, let us discuss how phase fluctuations do affect the observable fringe structure. Neglecting the contribution of $\Xi_1(p_x)$, the structure function shows maxima $\Xi_M = e^{-\mathcal{D}_\infty/2} (1 + \alpha)/(1 - \alpha)$ around the points $p_x = 2\ell\pi\hbar/d$ (ℓ integer), and minima $\Xi_m = e^{-\mathcal{D}_\infty/2} (1 - \alpha)/(1 + \alpha)$ in between. The contrast factor is defined as

$$Q(g, t) = (\Xi_M - \Xi_m)/(\Xi_M + \Xi_m) \quad (23)$$

($Q \sim 1$ means good contrast), while the peak width Γ , defined as the full width at half height between maxima and minima, is

$$\Gamma(g, t) = (4\hbar/d) \tan^{-1} [(1 - \alpha)/(1 + \alpha)]. \quad (24)$$

For $\Gamma \ll 2\pi\hbar/d$, i.e. when α is not far from its zero-temperature value $\alpha(g, 0) = 1$, the peaks are sharp and have a quasi-Lorentzian shape. However, Eq. (20) shows that the overall intensity is depressed by the factor $e^{-\mathcal{D}_\infty/2}$, which is plotted in Fig. 5 together with Q and Γ , for different coupling values: it appears that the main effect of quantum fluctuations is to weaken the overall intensity, while the contrast and the peak width are predominantly driven by temperature.

The authors wish to thank L. Pitaevskii and S. Stringari, as well as F. S. Cataliotti, F. Ferlaino, C. Fort, and M. Inguscio for useful discussions. This research is supported by the COFIN2000-MURST fund.

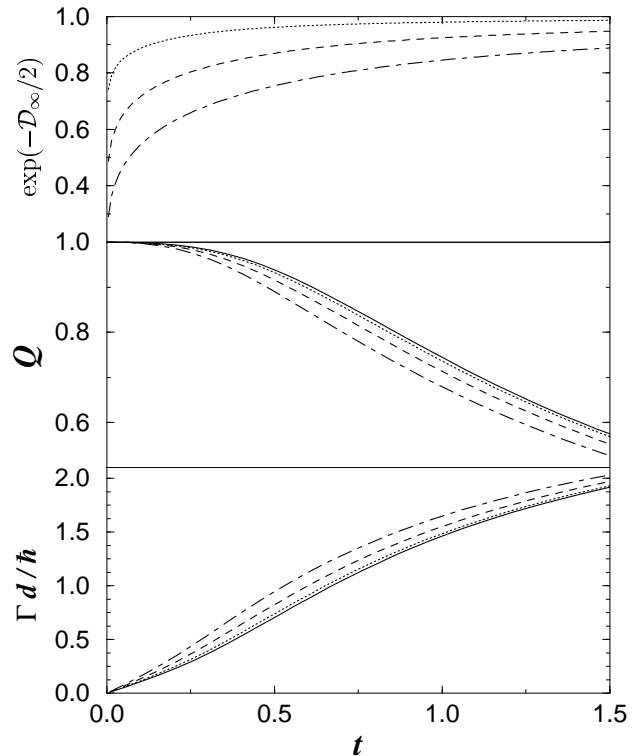


FIG. 5. Characteristics of the fringe structure $\Xi(p_x; g, t)$ of the 1D condensate array vs. temperature and for different values of the quantum coupling: $g = 0$ (solid lines, classical), $g = 1$ (dotted lines), $g = 2$ (dashed lines), and $g = 3$ (dash-dotted lines). Top: quantum attenuation factor $e^{-\mathcal{D}_\infty/2}$. Middle: contrast factor $Q(g, t)$, Eq. (23). Bottom: peak width $\Gamma(g, t)$, Eq. (24).

Stenger, S. Inouye, A. P. Chikkatur, D. M. Stamper-Kurn, D. E. Pritchard, and W. Ketterle, Phys. Rev. Lett. **82**, 4569 (1999); S. Burger, F. S. Cataliotti, C. Fort, F. Minardi, M. Inguscio, M. L. Chiofalo, M. P. Tosi, Phys. Rev. Lett. **86**, 4447 (2001).

⁵ A. Smerzi, S. Fantoni, S. Giovanazzi, and S. R. Shenoy, Phys. Rev. Lett. **79**, 4950 (1997); S. Raghavan, A. Smerzi, S. Fantoni, and S. R. Shenoy, Phys. Rev. A, **59**, 620 (1999); J. R. Anglin, P. Drummond, and A. Smerzi, cond-mat/0011440.

⁶ Anthony Leggett, Rev. Mod. Phys. **73**, 307 (2001).

⁷ S. W. Lovesey, RAL preprint 2001.

⁸ R. Giachetti and V. Tognetti, Phys. Rev. Lett. **55**, 912 (1985); Phys. Rev. B **33**, 7647 (1986).

⁹ See, e. g., A. Cuccoli, R. Giachetti, V. Tognetti, R. Vaia, and P. Verrucchi, J. Phys.: Condens. Matter **7**, 7891 (1995) and references therein.

¹⁰ A. Cuccoli, A. Fubini, V. Tognetti, and R. Vaia, Phys. Rev. E **60**, 231 (1999); Phys. Rev. B **61**, 11289 (2000).

¹¹ A. Cuccoli, V. Tognetti, and R. Vaia, Phys. Rev. A **44**, 2734 (1991); Phys. Lett. A **160**, 184 (1991).

¹² R. M. Bradley and S. Doniach, Phys. Rev. B **30**, 1138 (1984).

¹³ M. Greiner, I. Bloch, O. Mandel, T. W. Hänsch, and T. Esslinger, cond-mat/0105105.